Available online at www.sciencedirect.com
ScienceDirect
International Journal of Thermal Sciences 46 (2007) 426–433
International Journal of Thermal Sciences
www.elsevier.com/locate/ijts

A fractal model for critical heat flux in pool boiling ☆

Boqi Xiao, Boming Yu *

Department of Physics, Huazhong University of Science and Technology, 1037 Luoyu Road, Wuhan 430074, PR China

Received 10 March 2006; received in revised form 14 July 2006; accepted 14 July 2006

Available online 22 August 2006

Abstract

In this paper, a fractal model for the high heat flux nucleate boiling region and for the critical heat flux (CHF) is proposed. The expression for the critical heat flux (CHF) is derived based on the fractal distribution of nucleation sites on boiling surfaces. The proposed fractal model for CHF is found to be a function of wall superheat, the contact angle and physical properties of fluid. The relation between CHF and the number of active nucleation sites is obtained from the fractal distribution of active nucleation sites on boiling surfaces. The contact angle and the physical properties of fluid have the important effects on CHF. The predicted CHF from a boiling surface based on the proposed fractal model is compared with the existing experimental data. An excellent agreement between the proposed model predictions and experimental data is found.

Keywords: CHF; Pool boiling; Fractal; Heat transfer

1. Introduction

The mechanisms of CHF have been hotly debated in the past decades. The strong interest is due to practical applications since it is desirable to design an efficient heat exchanger or boiler to operate at as high heat flux as possible with optimum heat transfer rates without risk of physical burnout. There are many empirical correlations and models for CHF in the literature, with each applicable to a restricted range of experimental conditions. From a mechanistic viewpoint, although the influences of some parameters such as heater geometry, roughness of surfaces and contact angle etc. have extensively been discussed, an overall mechanistic description is still unavailable. In addition, each model/correlation has its disadvantages because of the limitations of experiment conditions. So, searching a comprehensive theory and unified model becomes a challenging task.

The CHF point is called the burnout point, at which the increased heat flux produced by a rise in temperature is offset by the increased resistance of the vapor blanket around the heater. Then, the temperature difference is low while the heat flux is very high. Heat transfer rates in this range are very high. However, it is very dangerous to run equipment near CHF. If heat flux q is raised beyond the upper limit, such a system will suffer a sudden and damaging increase of temperature.

The mechanism of CHF was one of the most controversial subjects for heat transfer in pool boiling in the past, and a variety of correlations and models for CHF were proposed. This paper focuses on the high heat flux nucleate boiling region and attempts to develop a fractal model for CHF. In the next section a brief review on the available models regarding CHF is addressed.

2. Some CHF models

Addoms [1] proposed that the buoyancy and thermal diffusivity of fluid were the controlling parameters for CHF, and he applied the dimensional analysis method and obtained the following correlation:

$$\frac{q_{CHF}}{\rho_g h_{fg}} = c_0 \left(\frac{g k_f}{\rho_f c_{pf}} \right)^{1/3} \tag{1}$$

where c_0 is a coefficient determined by the value of $(\rho_f - \rho_g)/\rho_f$.

☆ This work was supported by the National Natural Science Foundation of China through Grant number 10572052.

* Corresponding author.
E-mail address: yuboming2003@yahoo.com.cn (B. Yu).

1290-0729/$ – see front matter
doi:10.1016/j.ijthermalsci.2006.07.005

Nomenclature

C_{pf}	specific heat	$J\,kg^{-1}\,K^{-1}$
D	diameter	m
D_b	bubble departure diameter	m
D_s	spot diameter on surface	m
d_f	fractal dimension	
g	gravity acceleration	$m\,s^{-2}$
h_{fg}	latent heat of vaporization	$J\,kg^{-1}$
k_f	thermal conductivity	$W\,m^{-1}\,K^{-1}$
N_a	active nucleation site density	m^{-2}
$N_{a,\mathrm{tot}}$	total number of nucleation sites	
$\bar{N}$	average density of active nucleation	m^{-2}
q	heat flux	$W\,m^{-2}$
q_{CHF}	critical heat flux	$W\,m^{-2}$
R	radius	m
T	temperature	°C
T_s	saturation temperature	K
T_∞	bulk temperature	K
ΔT	wall superheat $(T_w - T_s)$	°C
t_w	bubble waiting time	s
t_g	bubble growth time	s

Greek symbols

α_f	thermal diffusivity	$m^2\,s^{-1}$
ρ	density	$kg\,m^{-3}$
ϕ	contact angle	°
γ	volumetric thermal expansion coefficient	K^{-1}
ν_f	kinematic viscosity	$m^2\,s^{-1}$
σ	surface tension	$N\,m^{-2}$
δ	thermal layer thickness	m
θ_s	D-value of $(T_s - T_\infty)$	°C
θ_w	D-value of $(T_W - T_\infty)$	°C

Subscripts

b	bubble
c	cavity
f	liquid phase
g	gas phase
max	maximum
min	minimum
nc	natural convection
s	saturation condition
tot	total
w	wall

Kutateladze [2] also applied the dimensional analysis of CHF based on the flooding mechanism and obtained the following relationship for the coefficient c as

$$c = \frac{q_{CHF}}{\rho_g^{1/2} h_{fg} [g\sigma(\rho_f - \rho_g)]^{1/4}} \tag{2}$$

He suggested that c was equal to 0.131 on the basic data from configurations other than infinite flat plates. The experimental data indicated that c was in the range of 0.13–0.16 for various liquids on wire and plate surfaces.

The bubble interference model was used by several researchers [3–5], and this model assumes that bubbles are impeded to be removed from the heating surfaces when heat flux reaches the CHF. This case is described by motion speed of bubbles. Based on energy balance, the latent heat flux of evaporation is entrapped by bubbles, which is the CHF when motion speed of bubbles reaches a critical value. The CHF is expressed as [5]

$$q_{CHF} = \frac{1}{2}\left(\frac{\pi}{6}\right)^{5/6} (0.0119\phi)^{1/2} h_{fg} \rho_g^{1/2} \left[2g\sigma(\rho_f - \rho_g)\right]^{1/4} \tag{3}$$

The coefficient c in Eq. (2) can be obtained by substituting Eq. (3) into Eq. (2). The coefficient c was found to be in the range of 0.17–0.24 if contact angles ϕ in the range of 46–60°.

Zuber and Westwater [6] proposed the hydrodynamic instability model, which was expressed as

$$0.15 > \frac{q_{CHF}}{h_{fg}\rho_g}\left[\frac{\rho_g^2}{\sigma g(\rho_f - \rho_g)}\right]^{1/4} > 0.12 \tag{4}$$

This CHF model is controlled by instability in the vapor–liquid interface of the vapor jets emanating from the heater surface during nucleate boiling. The onset of instability leads to breakdown in the process of vapor removal from the heater surface, eventually leading to complete vapor blanketing of the surface. In a power-controlled system, this causes the surface temperature to increase dramatically, whereas in a temperature-controlled system, this may cause a slight reduction in the heat flux. Kutateladze's model Eq. (2) was proved by Zuber, and this was Zuber's theoretical contribution.

The macrolayer dryout model was derived by Haramura and Katto [7] according to experimental observations and theoretical analysis. They proposed that the CHF occurs when the heat flux is sufficiently high to evaporate the macrolayer completely before liquid re-supply of the evaporating macrolayer. Thus the macrolayer was believed to be important to the process of boiling and possibly the CHF. The CHF can be expressed as [7]

$$q_{CHF} = \frac{t_{ev}}{t_{bg}} q_n \tag{5}$$

where t_{ev} is the average time of macrolayer dryout, t_{bg} is the re-supply time corresponding to the mushroom bubble's lifetime for simple geometries such as a horizontal flat plate, and q_n is the heat flux of macrolayer dryout for pool boiling. But the q_{CHF} given by Eq. (5) is lower than that from actual measurements.

Ha and No [8] derived a dry-spot model for CHF in pool boiling according to the Poisson distribution of active nucleation sites. The correlation is

$$q = q_b N_a \big(1 - P(n \geqslant n_c)\big) \tag{6a}$$

$$P(n) = \frac{e^{-N_a A}(N_a A)^n}{n!} \tag{6b}$$

$$P(0) = e^{-N_a A} \tag{6c}$$

$$q_b = \frac{q_{nb}}{N_a} \tag{6d}$$

where q_b is heat transferred by a single bubble site, q_{nb} is nucleate boiling heat flux, $P(n)$ is Poisson distribution, n is number of active nucleation sites, n_c is critical active site number which is 5, A is a shell area, N_a is the density of active nucleation sites, which will be discussed in Section 3 (see Eq. (15)).

Zhao et al. [9] derived a theoretical prediction for fully developed nucleate boiling based on a dynamic microlayer model in pool boiling. The correlation is expressed as

$$q_{CHF} = 4.5 \times 10^4 d^{-0.44} \tag{7a}$$

where d is the diameter of individual bubble at the end of initial growth. In order to determine d, Zhao et al. [9] applied Gaertner and Westwater's correlations [10]:

$$q = 117.1 N_a^{2/3} \tag{7b}$$

$$d = 17.8 q^{-0.75} \tag{7c}$$

Zuber et al. [11] pointed out that the formula of the CHF was derived which was the same as Eq. (2) from one of the following mechanisms:

(a) The accumulation and coalescence of vapor bubbles occur on wall surfaces and vapor stems interfere each other.
(b) Vapor phase of upward movement results in instability and split of liquid.
(c) Vapor phase of upward movement results in suspension or split of the micro liquid drop.

However, most of above theories have own disadvantage. The bubble interference model [3–5] was based on analysis of isolated bubble. However, it is well known that the accumulation and coalescence of bubbles cannot be neglected in CHF. The hydrodynamic instability model for CHF proposed by Zuber and Westwater [6] is determined by fluid mechanism strictly, which is a controversial problem and is independent of the state of surfaces. The macrolayer dryout model by Haramura and Katto [7] was derived according to experimental observation and theoretical analysis for mushroom vapor bubbles, but the macrolayer never is dry-out. So many researchers are suspicious of the theoretical foundation of the macrolayer dryout model. So far the mechanism of the CHF has been one of the most controversial subjects for heat transfer in pool boiling. There is no an available mechanistic description for the CHF. Although there are many correlations of CHF in the literature, each is applicable to a restricted range of experimental conditions.

3. Some correlations for predicting active nucleation site density

The density of active sites on heater surfaces is affected by the interaction of several parameters such as heater and liquid sides, distributions of cavities on heater surfaces and liquid–solid contact angles. At the same time, the transport properties of the heater affect the thermal interaction among the cavities, causing activation and deactivation of individual cavities. It has been shown that the density or number N_a of active nucleate sites on heated surfaces has the great effect on boiling heat transfer. Several studies have been performed on N_a, which give the functional dependence of N_a on q and ΔT. Here some notable studies are discussed in this field. Mikic and Rohsenow [12] might be the first to relate the active nucleation site density to the sizes of cavities present on the heated surfaces and expressed the functional dependence of active nucleation site density on cavity for commercial surfaces as

$$N_a \sim \left[\frac{D_{c,\max}}{D_c}\right]^m \tag{8a}$$

where $D_{c,\max}$ is the diameter of the largest cavity present on surfaces, m is an empirical constant ($= 6.5$) and D_c is given by

$$D_c = \frac{4\sigma T_S}{\rho_g h_{fg} \Delta T} \tag{8b}$$

Bier et al. [13], on the other hand, expressed N_a as a functional of cavity size from heat transfer data. The expression is given by

$$\ln N_a = \ln(N_{\max})\left[1 - \left(\frac{D_c}{D_{c,\max}}\right)^m\right] \tag{9}$$

where $N_{\max}$ is the value corresponding to $D_c = 0$. The value of the exponent m was found to depend on the surface preparation procedure.

Cornwell and Brown [14] made a systematic study on active nucleation site density of water boiling at 1.013 bars on a copper surface, with surface condition varying from smooth to rough, and related the dependence of active site density on wall superheat as

$$N_a \sim \Delta T^{4.5} \tag{10a}$$

They justified their observed functional dependence on wall superheat by assuming that only conical cavities exist on surfaces and that vapor needs to be trapped in cavities before any nucleation could occur. They also related the cavity size to the total number of cavities presenting on the surface from the cavity size data obtained by using an electron microscope, and $N_{a,\text{tot}}$ is expressed as

$$N_{a,\text{tot}} \sim \frac{1}{D_c^2} \tag{10b}$$

Yang and Kim [15] made the first attempt to quantitatively predict the active nucleation sites from knowledge of the size and cone angle distribution of cavities that are actually present on the surface. Using a scanning electron microscope and a differential inference contrast microscope, they established the dependence of the nucleation site density on the characteristic of a boiling surface with the aid of statistical analysis approach.

The size distribution was found to fit a Poisson distribution while a normal distribution was used for cone half angle β. They used Bankoff's [16] criteria to determine which cavities will trap gas. This condition is given by $\phi > 2\beta$. By combining the probability distribution functions and this criterion, they related N_a to the average $\bar{N}$ on the surface as

$$N_a = \bar{N} \int_{R_{\min}}^{R_{\max}} \lambda e^{-\lambda r}\,\mathrm{d}r \int_0^{\phi/2} \frac{1}{\sqrt{2\pi s}} \exp\left[-\frac{(\beta-\bar{\beta})^2}{2s}\right]\mathrm{d}\beta \tag{11}$$

where $\bar{\beta}$ is the mean value of cone half angle, and λ and s are statistical parameters. These parameters are dependent upon the surface preparation procedure and the material of surface.

Kocamustafaogullari and Ishii [17] developed a relation for active nucleation site density in pool boiling. Their correlation expressed active nucleation site density as a function of dimensionless minimum cavity size and density ratio. The correlation for system pressures from 1.0 to 198.0 bars is

$$N_a^* = f(\rho^*) r_c^{*-4.4} \tag{12}$$

where $N_a^* = N_a D_d^2$, $r_c^* = 2r_c/D_d$, $r_c = 2\sigma T_s/\rho_f h_{fg} \Delta T$, $\rho^* = (\rho_f - \rho_g)/\rho_g$, $D_d = 0.0012(\Delta\rho/\rho_g)^{0.9} D_{dF}$, $f(\rho) = 2.157 \times 10^{-7}\rho^{*-3.2}(1 + 0.0049\rho^*)^{4.13}$ is density function, and D_{dF} is the Fritz diameter given as $D_{dF} = 0.0208\phi[\sigma/g(\rho_f - \rho_g)]^{1/2}$.

Jakob [18] first reported the relationship between N_a and q. However, his observations were limited to the cases of low heat flux because at high heat flux bubbles at neighboring sites start to merge; the merge of bubbles obscures the determination of the sites that are active underneath a large bubble. Gaertner and Westwater [10] employed a novel technique in which nickel salts were dissolved in water and the heater surface acted as one of the electrodes. By counting the numbers of holes in the deposited layer, they found the functional dependence of active nucleation site density on wall heat flux to be

$$N_a \sim q^{2.1} \tag{13}$$

Paul and Abdel-Khalik [19] conducted their experiments on the pool boiling of saturated water at 1 atm along an electrically heated horizontal platinum wire. Using high-speed photography, they measured active nucleation site density and bubble departure diameter up to 70%. They found that the active nucleation site density of N_a can be represented by the linear relationship with the boiling heat flux as follows:

$$N_a = 1.207 \times 10^{-3} q + 15.74 \tag{14}$$

Wang and Dhir [20] might be the first to perform a systematic study of the effect of contact angle on the density of active nucleation sites. The correlated cavity size D_c was related to the wall superheat for nucleation as given by Eq. (8b). It was found that there was a strong influence of wettability on active nucleation site density. For surfaces with $18^\circ \leqslant \phi \leqslant 90^\circ$, they correlated N_a with D_c as

$$N_a = 5.0 \times 10^5 (1 - \cos\phi) D_c^{-6} \tag{15}$$

It is clear that so far the available models for N_a and q are usually correlated with several empirical constants which have no physical meanings, and the mechanisms behind these constants are still not clear until now. Therefore, a complete mechanistic description for N_a and q is desirable from a mechanistic viewpoint. The next section will focus on the description of N_a based on the fractal distribution of nucleation sites present on heat surfaces.

4. Fractal analysis of nucleation sites on a boiling surface for CHF

This work is devoted to deriving a CHF model based on the fractal distribution of nucleation sites N_a on heat surfaces. We consider the active cavities formed on the heated surface to be analogous to pores in porous media. Yu and Cheng [21] found that the cumulative number of pores in porous media with the diameter greater than and equal to a particular value, D_s, obeys the following fractal scaling law

$$N(D_L \geqslant D_s) = (D_{s,\max}/D_s)^{d_f} \quad \text{with } D_{s,\min} \leqslant D_s \leqslant D_{s,\max} \tag{16a}$$

where $D_{s,\max}$ is the maximum diameter of pores in porous media, D_s is the diameter of a pore, and d_f is the area fractal dimension. If active cavities formed on surface are considered as pores in porous media, the cumulative number of active cavities with diameters greater than and equal to D_c is also described by Eq. (16a) with N and D_s replaced by N_a and D_c respectively, i.e.,

$$N_a(D_L \geqslant D_c) = (D_{c,\max}/D_c)^{d_f} \quad \text{with } D_{c,\min} \leqslant D_c \leqslant D_{c,\max} \tag{16b}$$

Eq. (16b) also implies that cavities acting as bubble emitting centers actually are statistically self-similar. The total number of nucleation sites from the minimum active cavity to the maximum active cavity can be obtained from Eq. (16b) as

$$N_{a,\mathrm{tot}} = \left(\frac{D_{c,\max}}{D_{c,\min}}\right)^{d_f} \tag{17}$$

The minimum active cavity radius $R_{\min}$ and the maximum active cavity radius $R_{\max}$ could be predicted by Hsu's model [22]:

$$R_{\min} = \frac{\delta}{C_1}\left[1 - \frac{\theta_s}{\theta_w} - \sqrt{\left(1 - \frac{\theta_s}{\theta_w}\right)^2 - \frac{4\zeta C_3}{\delta\theta_w}}\right] \tag{18a}$$

$$R_{\max} = \frac{\delta}{C_1}\left[1 - \frac{\theta_s}{\theta_w} + \sqrt{\left(1 - \frac{\theta_s}{\theta_w}\right)^2 - \frac{4\zeta C_3}{\delta\theta_w}}\right] \tag{18b}$$

where $\zeta = \frac{2\sigma T_s}{\rho_g h_{fg}}$, $C_1 = \frac{(1+\cos\phi)}{\sin\phi}$ and $C_3 = 1 + \cos\phi$, with ϕ being the contact angle of the fluid and the heater material, $D_{c,\max} = 2R_{\max}$, $D_{c,\min} = 2R_{\min}$. δ is the thermal boundary layer thickness which can be usually expressed as

$$\delta = \frac{k_f}{h_{nc}} \tag{19}$$

where h_{nc} is the average heat transfer coefficient for natural convection. For turbulence, Han and Griffith [23] applied the following correlation:

$$h_{nc} = 0.14\rho_f c_{pf}\left[\frac{\gamma g(T_w - T_\infty)\alpha_f^2}{\upsilon_f}\right] \tag{20}$$

If Eq. (20) is substituted into Eq. (19), the thermal boundary layer δ can be obtained from Eq. (19).

Hsu [22] pointed out that a cavity can be active in the range of $R_{\min} < R < R_{\max}$. A cavity can be ineffective at low wall temperature (or low heat flux).

In nucleate pool boiling, the fractal dimension d_f of nucleation sites is given by Yu and Cheng [24] as

$$d_f = \ln\left[\frac{1}{2}\left(\frac{\bar{D}_{c,\max}}{D_{c,\min}}\right)^2\right] \Big/ \ln\frac{D_{c,\max}}{D_{c,\min}} \tag{21}$$

where $\bar{D}_{c,\max}$ is the averaged value over all the maximum active cavities as

$$\bar{D}_{c,\max} = \frac{1}{(T_w - T_s)}\int_{T_s}^{T_w} D_{c,\max}(T_w)\,\mathrm{d}T_w = \frac{1}{\Delta T}\sum_{j=1}^{m} D_{c,\max}(T_{w_j})\delta T_w = \frac{1}{m}\sum_{j=1}^{m} D_{c,\max}(T_{w_j}) \tag{22}$$

where $m = \Delta T/\delta T_w$, and a constant δT_w is assumed. In the above equation, $T_{w_j} = T_s + j(\delta T_w)$ with $j = 1, 2, \ldots, m$. For example, if we choose $\delta T_w = 0.2\,^\circ\mathrm{C}$ then $m = 5$ for $\Delta T = 1\,^\circ\mathrm{C}$, and $m = 50$ for $\Delta T = 10\,^\circ\mathrm{C}$.

Fig. 1(a) is an image of nucleation sites for the contact angle $\phi = 90^\circ$ as $q = 5.7 \times 10^5\ \mathrm{W\,m^{-2}}$ approaches CHF with a heating area of 2.5 cm^2, which was taken from Wang and Dhir's experiment data [20]. A linear relationship on the logarithmic scale exists as shown in Fig. 1(b) if the box-counting method [25] is applied to the photo image. The fractal dimensional d_f of size (area) of the nucleation sites can be determined from the slope to be 1.83 [24]. It confirms that the nucleation sites follow the fractal scaling law by Eq. (16), which shows that the cavities, acting as bubble emitting centers, are self-similar.

Fig. 2 is a plot of the fractal dimension versus wall superheat for $\phi = 90^\circ$. According to the fractal geometry theory, the fractal dimension d_f should be in the range of $1 < d_f < 2$ in two dimensions. Fig. 2 shows that the fractal dimension d_f is in the range of $1 < d_f < 2$ when wall superheat is given in the range of $12\,^\circ\mathrm{C} \leqslant \Delta T \leqslant 35\,^\circ\mathrm{C}$ for contact angle $\phi = 90^\circ$. For a water–copper system with a contact angle $\phi = 90^\circ$, it was found from Eq. (21) that $d_f > 1.82$ when the wall superheat $\Delta T > 12\,^\circ\mathrm{C}$. This means that the number of active nucleate sites versus sizes is fractal if they are in the wall superheat as specified above. Fig. 2 also shows that the fractal dimension increases with wall superheat. This means that d_f is a function of wall superheat. Eq. (21) gives $d_f = 1.85$ for $\phi = 90^\circ$ at $\Delta T = 18\,^\circ\mathrm{C}$. The datum point of $d_f = 1.83$ at $\Delta T = 18\,^\circ\mathrm{C}$ for $\phi = 90^\circ$ obtained based on the box-counting method from Fig. 1(a) is also included in Fig. 2 for comparison purpose. It can be seen from Fig. 2 that at $\Delta T = 18\,^\circ\mathrm{C}$ there is an error of about 1% between the present model predictions and the experimental data.

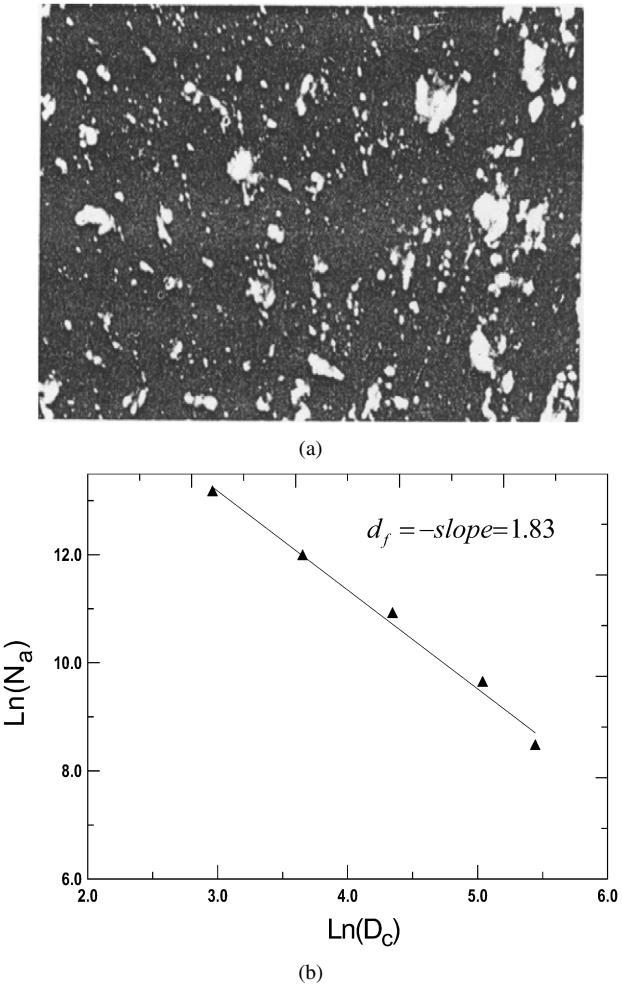

Fig. 1. (a) A photograph [20] of active nucleation sites for $\phi = 90^\circ$ as $q = 5.7 \times 10^5\ \mathrm{W\,m^{-2}}$ approaches CHF, and (b) determination of fractal dimension of nucleation sites from (a).

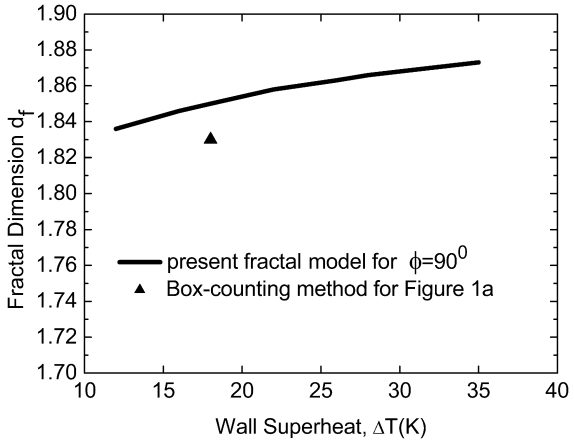

Fig. 2. Fractal dimension versus wall superheat for $\phi = 90^\circ$.

5. The fractal model for CHF

Kenning and Del Valle [26] showed that the interference between bubbles has little effect on heat transfer in fully-developed nucleate boiling. Thus the effect of overlap between bubbles is assumed to be not large and is ignored in this work.

In addition, according to Haramura and Katto [7]'s macrolayer dryout model, the dominant heat transfer is attributed to the evaporation of fluid. Zhao et al. [9] also pointed out that the heat transferred from the surface is used to evaporate the fluid, and this evaporation plays a dominant role in fully developed nucleate boiling regions, including the CHF. Pasamehmetoglu et al. [27] also applied the Haramura and Katto [7]'s macrolayer dryout model to analyze the heat transfer dominated by the evaporation of fluid. Therefore, to simplify the modeling of the CHF phenomena, in this fractal mode we also assume that all the heat transferred from the surface is used to evaporate the fluid.

If the bubbles formed at active sites on the heating surface leave the surface with average volume V_b and average departure frequency f, the heat transfer as a result of bubble formation at high heat flux region may be obtained as

$$q = h_{fg}\rho_g V_b f N_a \tag{23}$$

where f is the bubble average departure frequency, V_b is the average volume of single bubble which is usually expressed as

$$V_b = \frac{\pi}{6} D_b^3 \tag{24}$$

where D_b is the bubble departure diameter, which is given by Fritz [28] as

$$D_b = 0.0208\phi \sqrt{\frac{\sigma}{g(\rho_f - \rho_g)}} \tag{25}$$

It is evident that the bubble departure diameter D_b is proportional to the contact angle and fluid properties. This model for the bubble departure diameter for CHF was also applied by some other researchers [3–5].

Conventionally, N_a in Eq. (23) is related to the active cavity diameter or heat flux by a variety of correlations with several empirical constants, such as Eqs. (8)–(15). However, no generally accepted model for N_a has been available so far. This work attempts to modify Eq. (23) and derive a fractal model for CHF.

In the following, a fractal model for CHF is derived based on the fact that the nucleation site size distribution follow the fractal power law given by Eq. (16b). The number of active cavities of sizes lying between D_c and $D_c + \mathrm{d}D_c$ can be obtained from Eq. (16b) as

$$-\mathrm{d}N_a = d_f D_{c,\max}^{d_f} D_c^{-(d_f+1)}\,\mathrm{d}D_c \tag{26}$$

where $\mathrm{d}D_c > 0$ and $-\mathrm{d}N_a > 0$, which means that the nucleation site number decreases with the increase of the diameter of active cavities.

It is also clear that the heat removed from the wall surface by a single bubble is

$$c_q = h_{fg}\rho_g V_b = \pi h_{fg}\rho_g D_b^3/6 \tag{27a}$$

where V_b is expressed by Eq. (24). Since the nucleation site sizes are non-uniform and follow the fractal power law Eq. (16b), the heat transferred by the nucleation sites (through bubbles) between D_c and $D_c + \mathrm{d}D_c$ can be written as

$$\mathrm{d}q = -c_q f\,\mathrm{d}N_a \tag{27b}$$

where f is the bubble release frequency, which is also related to the nucleation site size D_c and will be discussed later, and $(-\mathrm{d}N_a)$ is given by Eq. (26). The total heat transferred by all nucleation sites from the minimum site $D_{c,\min}$ to the maximum site $D_{c,\max}$ can be obtained by

$$q = \int \mathrm{d}q = -\int_{D_{c,\min}}^{D_{c,\max}} c_q f\,\mathrm{d}N_a \tag{27c}$$

It is expected that those empirical constants in Eqs. (8)–(15) will not appear in the result of the integration of Eq. (27c). Eq. (27c) indicates that the total heat flux depends on the active site sizes, the bubble departure frequency f as well as the bubble departure diameter D_b. The higher the number of active sites, the higher the heat flux q; the higher the bubble departure frequency f, the higher the heat flux q; and the larger the bubble departure diameter D_b, the higher the heat flux q. These are expected and are consistent with the practical situations. Eq. (27c) can be integrated if the bubble departure diameter f is expressed in terms of D_c. To this end, we note that the bubble departure frequency, f, is usually expressed as

$$f = \frac{1}{t_w + t_g} \tag{28}$$

where t_w is the bubble waiting time, t_g is the bubble growth time. In pure liquids, Van Stralen et al. [29] assumed that the waiting time is related to the growth time by

$$t_w = 3t_g \tag{29}$$

Han and Griffith [23] obtained the analytical expression for the bubble waiting time, t_w, which is related to the cavity size $(D_c = 2R_c)$ by

$$t_w = \frac{9}{4\pi\alpha_f}\left[\frac{(T_w - T_\infty)R_c}{T_w - T_s(1 + 2\sigma/R_c\rho_g h_{fg})}\right]^2 \tag{30}$$

where R_c is the cavity radius. On a copper surface, Wang and Dhir's [20] measured $R_c = 1.1$–27.7 μm for pool boiling of saturated water at 1 atm pressure. A rough estimation of the term $2\sigma/R_c\rho_g h_{fg}$ gives 0.1–0.01 for $R_c = 1.0$–10 μm. So in Eq. (30) the term $2\sigma/R_c\rho_g h_{fg}$ can be neglected for the simplicity of integration, and Eq. (30) can be reduced to

$$t_w = \frac{9}{16\pi\alpha_f}\left(\frac{T_w - T_\infty}{\Delta T}\right)^2 D_c^2 \tag{31}$$

Eq. (31) indicates that the larger the active cavity, the longer the waiting time, which is consistent with the physical phenomena. It should be noted that in Eq. (31) the bulk temperature should not be set to equal the saturation temperature. Substituting Eqs. (31) and (29) into Eq. (28) for the bubble departure frequency f, we can see that the bubble departure frequency, f, is related to the sizes of active cavities. Eq. (27c) can now be integrated to give

$$q = -\int_{D_{c,\min}}^{D_{c,\max}} c_q f\,\mathrm{d}N_a$$

$$= \int_{D_{c,\min}}^{D_{c,\max}} c_q \frac{4\pi\alpha_f}{3}\left(\frac{\Delta T}{T_w - T_\infty}\right)^2 D_c^{-2} d_f D_{c,\max}^{d_f} D_c^{-(d_f+1)}\,\mathrm{d}D_c$$

$$= c_q \frac{d_f}{d_f+2}\frac{4\pi\alpha_f}{3}\left(\frac{\Delta T}{T_w - T_\infty}\right)^2 D_{c,\max}^{-2}\left[(N_{a,\mathrm{tot}})^{1+2/d_f} - 1\right] \tag{32}$$

Eq. (32) denotes that the high heat flux and CHF are a function of wall superheat, fractal dimension, contact angle and physical properties of fluid, and no additional parameter is introduced in this model. It is expected that Eq. (32) has less empirical constants than the conventional models, and every parameter in Eq. (32) has clear physical meaning.

6. Comparison with CHF data in pool boiling

Wang and Dhir [20] conducted experiments on the pool boiling of saturated water at 1 atm on a vertical rectangular copper surface. We now compare the results obtained from the present fractal model with the experimental results by Wang and Dhir [20]. Their high heat flux data for contact angle $\phi = 18°$ is presented in Fig. 3. The solid line in Fig. 3 represents the predictions by the present fractal model with the value of d_f computed from Eq. (21). In Fig. 3 the highest point is point D, which is CHF point. The results show that the CHF from the present fractal model is in excellent agreement with Wang and Dhir's experimental observation [20]. Fig. 4 shows a comparison among the present model predictions, Dhir and Liaw's experimental data [30], Zuber's model [31] for CHF and Ha and No's correlation Eq. (6) [8] at contact angle $\phi = 14°$. It is seen from Eq. (6) that Ha and No's correlation [8] contains two empirical constants $n_c = 5$, and the value of 5.0×10^5 which is associated with Eq. (15). Fig. 4 shows that the fractal model predictions are quite satisfactory, and the predicted CHF is found to be in good agreement with the others, especially for the high heat flux. In Gaertner and Westwater's experiments [10], nickel salts were dissolved in water and boiling was observed on a 5-cm-dia horizontal copper surface. Fig. 5 denotes a comparison among the present model predictions, Gaertner and Westwater's experimental data [10] and Zhao et al.'s correlation Eq. (7a) [9] at contact angle $\phi = 22°$. But Eq. (7) contains six empirical constants. Fig. 5 indicates that the present model predictions are found to be in good agreement with the others at the high heat flux. Table 1 compares the predicted high heat flux by the present model with the data by Gaertner and Westwater [10]. It can be seen from Table 1 that at high wall superheat an error of about 3% exists between the present model predictions and the experimental data. Fig. 6 compares the present model predictions for CHF with Hahne and Diesselhorst 's experimental data [32] for Al and NiCr surfaces. The figure shows that the model predictions are again found to be in good agreement with the experimental data. The figure also indicates that the contact angle has the significant influence on CHF.

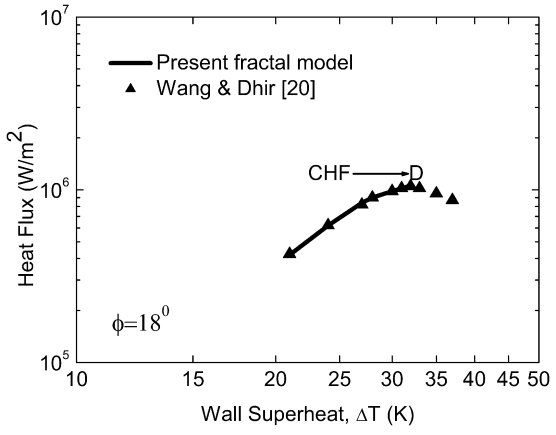

Fig. 3. A comparison between the fractal model predictions and experimental data at contact angle $\phi = 18°$.

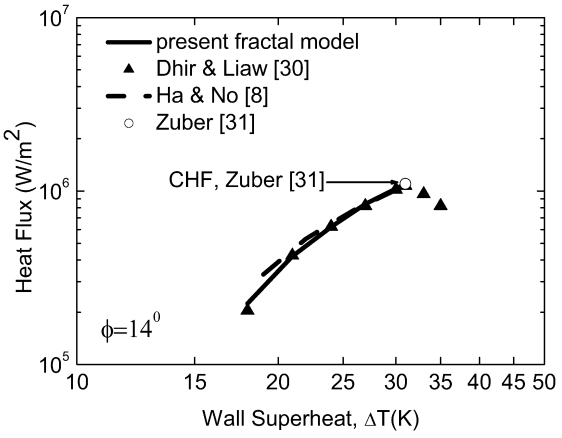

Fig. 4. A comparison between the fractal model predictions and experimental data at contact angle $\phi = 14°$.

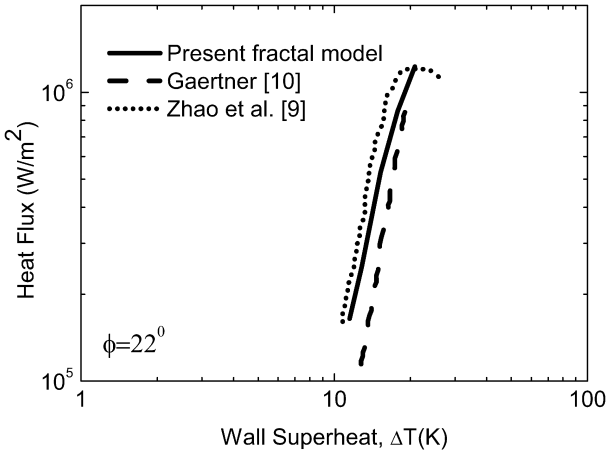

Fig. 5. A comparison between the fractal model predictions and experimental data at contact angle $\phi = 22°$.

Table 1
A comparison of the high heat flux between the present model and the experimental data at $\phi = 8°$ by Gaertner and Westwater [10]

$\Delta T(K)$	Present model at $\phi = 8°$ q [W cm^{-2}]	Experimental data [10] q [W cm^{-2}]
25	53	44
30	99	96

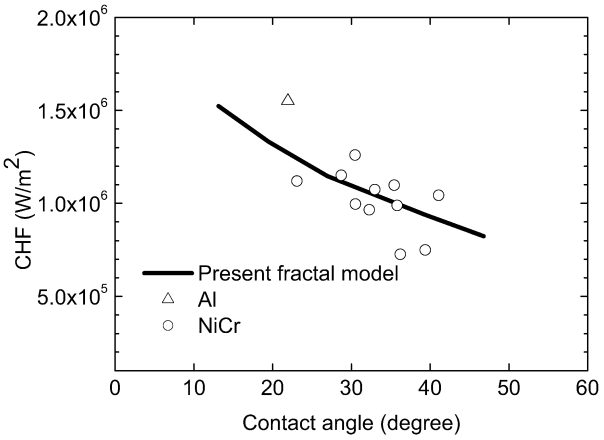

Fig. 6. A comparison between the present model predictions and the experimental data [32] for the influence of contact angle on CHF.

7. Summary and conclusion

A fractal model for the CHF is derived based on the fractal distribution of active nucleation sites on boiling surfaces. The proposed model is expressed as a function of area (size) fractal dimension of active nucleation sites, maximum and minimum active cavities, wall superheat, the contact angle, and physical properties of fluid. No additional empirical constant is introduced. This fractal model contains less empirical constants than the conventional correlations. The predicted CHF based on the proposed fractal model is shown to be in excellent agreement with experiment data.

References

[1] J.N. Addoms, Heat transfer at high rates to water boiling outside cylinder, DSc thesis, Chem. Eng. Department, MIT, June, 1948.
[2] S.S. Kutateladze, A hydrodynamic theory of changes in boiling process under free convection, Izv. Akademia Nauk Otdeleme Tekh. Nauk 4 (1951) 529–536.
[3] R.G. Deissler, Columbia University Heat Transfer Symposium, New York, 1954.
[4] W. Rohsenow, P. Griffith, Chem. Engrg. Progr. Symp. Ser. 52 (18) (1956) 47–49.
[5] Y.P. Chang, N.W. Snyder, Heat transfer in saturated boiling, Chem. Engrg. Progr. Symp. Ser. 56 (30) (1960) 25–28.
[6] N. Zuber, J.W. Westwater, The hydrodynamic crisis in pool boiling of saturated and subcooled liquids, in: 2nd Int. Heat Trans Conf., Denver, 1961, p. 27.
[7] Y. Haramura, Y. Katto, A new hydrodynamic model of critical heat flux, applicable widely to boiling to both pool and forced convection boiling on submerged bodies in saturated liquid, Int. J. Heat Mass Transfer 26 (3) (1983) 389–399.
[8] S.J. Ha, H.C. No, A dry-spot model of critical heat flux in pool and forced convection boiling, Int. J. Heat Mass Transfer 41 (2) (1998) 303–311.
[9] Y.H. Zhao, T. Masuoka, T. Tsuruta, Unified theoretical prediction of fully developed nucleate boiling and critical heat flux based on a dynamic microlayer model, Int. J. Heat Transfer 45 (2002) 3189–3197.
[10] R.F. Gaertner, J.W. Westwater, Population of active sites in nucleate boiling heat transfer, Chem. Engrg. Progr. Symp. Ser. 56 (1960) 39–48.
[11] N. Zuber, M. Tribus, J.W. Westwater, Hydrodynamic crisis in pool boiling of saturated and subcooled Liquids, author' reply, Int. Heat Transfer Conf. Discussion D-84–D-94 (1962).
[12] B.B. Mikic, W.M. Rohsenow, A new correlation of pool boiling data including the effect of heating surface characteristic, Trans. ASME. J. Heat Mass Transfer 91 (1969) 245–250.
[13] K. Bier, D. Gorenflo, M. Salem, Y. Tanes, Pool boiling heat transfer and size of active nucleation centers for horizontal plates with different surface roughness, in: Proceedings of 6th International Heat Transfer Conference, Toronto, vol. 1, 1978, pp. 151–156.
[14] K. Cornwell, R.D. Brown, Boiling surface topography, in: Proceedings of 6th International Heat Transfer Conference, Toronto, vol. 1, 1978, pp. 157–161.
[15] S.R. Yang, R.H. Kim, A mathematical model of pool boiling nucleation site density in terms of surface characteristics, Int. J. Heat Mass Transfer 31 (1988) 1127–1135.
[16] S.G. Bankoff, Entrapment of gas in spreading of liquid over a rough surface, AIChE J. 4 (1958) 24–26.
[17] G. Kocamustafaogullari, M. Ishii, Interfacial area and nucleation site density in boiling systems, Int. J. Heat Mass Transfer 26 (9) (1983) 1377–1387.
[18] M. Jakob, Heat Transfer, Wiley, New York, 1949.
[19] D.D. Paul, S.I. Abdel-Khalik, A statistical analysis of saturated nucleate boiling along a heated wire, Int. J. Heat Mass Transfer 26 (4) (1983) 509–519.
[20] C.H. Wang, V.K. Dhir, Effect of surface wettability on active nucleation site density during pool boiling of water on a vertical surface, ASME J. Heat Transfer 115 (1993) 659–669.
[21] B.M. Yu, P. Cheng, Fractal models for the effective thermal conductivity of bidispersed porous media, AIAA J. Thermophys. Heat Transfer 16 (1) (2002) 22–29.
[22] Y.Y. Hsu, On the size range of active nucleation cavities on a heating surface, J. Heat Transfer 84 (1962) 207–215.
[23] C.Y. Han, P. Griffith, The mechanism of heat transfer in nucleate pool boiling—Part I and II, Int. J. Heat Mass Transfer 8 (1965) 887–913.
[24] B.M. Yu, P. Cheng, A fractal model for nucleate pool boiling heat transfer, ASME J. Heat Transfer 124 (2002) 1117–1124.
[25] J. Feder, Fractals, Plenum, New York, 1988.
[26] D.B.R. Kenning, M.V.H. Del Valle, Fully developed nucleate boiling: overlap of areas of influence and interference between bubble sites, Int. J. Heat Mass Transfer 24 (6) (1981) 1025–1032.
[27] K.O. Pasamehmetoglu, P.R. Chappidi, C. Unal, R.A. Nelson, Saturated pool nucleate boiling mechanisms at high heat fluxes, Int. J. Heat Mass Transfer 36 (1993) 3859–3868.
[28] W. Fritz, Maximum volume of vapor bubbles, Physik Zeitschr. 36 (1935) 379–384.
[29] S.J.D. Van Stralen, M.S. Sohan, R. Cole, W.M. Sluyter, Bubbles growth rates in pure and binary systems: Combined effect of relaxation and evaporation microlayers, Int. J. Heat Transfer 18 (1975) 453–467.
[30] V.K. Dhir, S.P. Liaw, Framework for a united model for nucleate and transition pool boiling, ASME J. Heat Transfer 111 (1989) 739–746.
[31] N. Zuber, Stability of boiling heat transfer, ASME J. Heat Transfer 80 (1958) 711–720.
[32] E. Hahne, T. Diesselhorst, Hydrodynamic and surface effects on the peak heat flux in pool boiling, in: Proc. 6th Int. Heat Transfer Conference, Toronto, vol. 1, 1978.